

# A Fractional Order Controller Design Based on Bode's Ideal Transfer Function and Bode's Ideal Cut-Off Ideas

WeiJia Zheng\* Ying Luo\*\* YangQuan Chen\*\*\*

\* School of Automation, Foshan University, Foshan, China, (e-mail: z.wj08@mail.scut.edu.cn)

\*\* 1. Department of Mechanical Science and Engineering, Huazhong University of Science and Technology, Wuhan, Hubei Province, China,  
2. School of Automation, Foshan University, Foshan, China, (e-mail: ying.luo@hust.edu.cn)

\*\*\* School of Engineering, University of California, Merced, 5200 North Lake Road, Merced, CA, USA, (email: ychen53@ucmerced.edu)

---

**Abstract:** In order to improve the anti-load disturbance performance of a class of motion control systems, an improved fractional order controller design based on the Bode's ideal transfer function (BITF) is proposed in this paper. By adding a proportional-integral (PI) controller and a Bode's ideal cut-off (BICO) filter into the existing BITF based controller, the frequency characteristics of the control system in the low and high frequency ranges are improved without affecting the characteristics in the middle frequency range. Therefore, the steady-state accuracy and anti-disturbance performance of the system can be improved. A tuning method for the improved BITF based controller is proposed, using which the controller parameters can be obtained through simple calculation. The step response and disturbance rejection performance of the improved BITF based control system is illustrated by motion control simulation. Besides, the advantage of the proposed method is verified by the comparisons with some existing methods.

*Keywords:* fractional order controller, Bode's ideal transfer function, Bode's ideal cut-off filter, PID control, motion control

---

## 1. INTRODUCTION

In the last decade, there are soaring research and reports of fractional calculus in modeling and control area (Padula and Visioli (2011), Malek et al. (2016), Li et al. (2017)). Compared with the conventional integer-order calculus, fractional calculus has the potential to provide more realistic description of the real-world systems (Zheng et al. (2016), Tian et al. (2019)) and more options for the controller design (Monje et al. (2008), Bigdeli (2015)). However, the tuning of the fractional order controller is also becoming more and more complicated.

A commonly used fractional order controller is the fractional order  $PI^\lambda D^\mu$  controller, which is an extension of the traditional integer-order PID controller. Due to the extended value range, the  $PI^\lambda D^\mu$  controller can offer better control performance of control systems (Podlubny (1999), Shah and Agashe (2016)). Derived from the  $PI^\lambda D^\mu$  controller, the controller based on the Bode's ideal transfer function (BITF) (Bode (1945)) is another kind of fractional order controller. The controller is designed by shaping the open-loop frequency characteristic curve of the control system to be close to the shape of the Bode's ideal transfer function (Al-Saggaf et al. (2016), Azarmi et al. (2016)). Thus, applying the BITF based controller, the characteristic of the obtained control system can be directly specified (Patil et al. (2015), Yumuk et al. (2019)).

However, the existing BITF based controller may not offer the satisfied anti-load disturbance performance for motion control systems. In this paper, an improved BITF based controller is proposed to improve the anti-load disturbance performance of a class of motion control systems. By adding a proportional-integral (PI) controller and a Bode's ideal cut-off (BICO) filter (Luo et al. (2013)) into the existing BITF based controller, the amplitude characteristic of the control system is improved, while that in the middle frequency range is reserved. Besides, the tuning method for the improved BITF based controller is proposed, according to which the controller parameters can be calculated analytically. Motion control simulation is performed to test the gain robustness, step response and anti-load disturbance performance of the improved BITF based control system. The advantage of the improved BITF based controller is demonstrated by the comparisons with some existing control methods.

## 2. IMPROVED BITF BASED CONTROLLER

The Bode's ideal transfer function (Bode (1945)) can be represented as

$$G_B(s) = \left(\frac{\omega_c}{s}\right)^\xi, \quad (1)$$

where  $\omega_c$  represents the gain crossover frequency, and  $\xi$  represents a real number specifying the slope of the

amplitude curve and the phase of the system, which can be derived from the phase margin  $\varphi_m$ ,

$$\xi = 2 \left( 1 - \frac{\varphi_m}{\pi} \right). \quad (2)$$

Then the slope of the magnitude characteristic curve is  $-20\xi\text{dB/dec}$ .

Given  $\omega_c = 40\text{rad/s}$ ,  $\varphi_m = 50^\circ$ , the Bode plot of the Bode's ideal transfer function is shown in Fig. 1. It can be seen that the amplitude curve is a straight line, while the phase curve is a horizontal line.

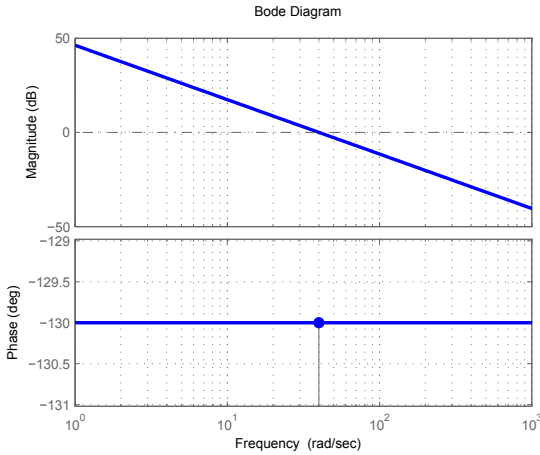


Fig. 1. The open Bode plot of the Bode's ideal transfer function with  $\omega_c = 40\text{rad/s}$  and  $\varphi_m = 50^\circ$

The typical feedback control system is represented as Fig. 2, where  $r$  and  $y$  are the reference and output signals, respectively,  $G(s)$  and  $C(s)$  are the plant model and controller, respectively.

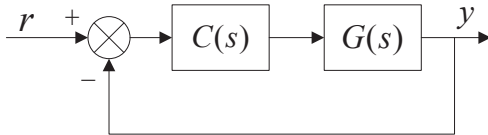


Fig. 2. The typical feedback control system

The plant model  $G(s)$  has the form represented by (3),

$$G(s) = \frac{K}{as^\alpha + bs^\beta + c}, \quad (3)$$

where  $a$ ,  $b$ ,  $c$  and  $K$  are model parameters,  $\alpha$  and  $\beta$  are fractional orders, respectively,  $\alpha \in (1, 3)$ ,  $\beta \in (0, 2)$ .

Taking the Bode's ideal transfer function as the open-loop transfer function of the control system shown in Fig. 2, yields

$$C(s)G(s) = \frac{C(s)K}{as^\alpha + bs^\beta + c} = \left( \frac{\omega_c}{s} \right)^\xi, \quad (4)$$

Therefore, the BITF based controller can be obtained,

$$C(s) = \frac{b\omega_c^\xi}{K} \frac{1}{s^{\xi-\beta}} \left( 1 + \frac{c}{bs^\beta} + \frac{a}{b}s^{\alpha-\beta} \right). \quad (5)$$

The BITF based controller is formed by a  $\text{PI}^\lambda\text{D}^\mu$  controller and a fractional order integrator connected in cascade.

Based on the design indices and model parameters, the controller parameters can be obtained through simple calculation.

According to (5), if the BITF based controller is applied to a class of motion control systems, whose parameter  $c$  is 0, the  $\text{PI}^\lambda\text{D}^\mu$  controller in the BITF based controller will become a  $\text{PD}^\mu$  controller. Thus, the steady-state accuracy and disturbance rejection of the control system rely on the fractional order integrator  $1/s^{\xi-\beta}$ . In order to guarantee good steady-state accuracy and disturbance rejection,  $\xi$  should be large enough to obtain sufficient integral effect. However, according to (2), the increase of  $\xi$  will lead to the decrease of the control system's phase margin.

In order to solve this problem, a PI controller is introduced to improve the steady-state accuracy and disturbance rejection performance of the control system, without affecting the system's stability. Besides, a Bode's ideal cut-off (BICO) filter (Luo et al. (2013)) is also introduced to enhance the high-frequency noise rejection of the control system. Therefore, an improved Bode's ideal transfer function is proposed,

$$L(s) = G_f(s) \left( \frac{\omega_c}{s} \right)^\xi G_{\text{BICO}}(s), \quad (6)$$

where  $G_f(s)$  is a PI controller,

$$G_f(s) = 1 + \frac{1}{T_1 s}, \quad (7)$$

where  $T_1$  represents the integral time constant. Besides,  $G_{\text{BICO}}(s)$  is a BICO filter,

$$G_{\text{BICO}}(s) = \frac{1}{\left( \sqrt{1 + \left( \frac{s}{\omega_{cf}} \right)^2} + \frac{s}{\omega_{cf}} \right)^r}, \quad (8)$$

where  $\omega_{cf}$  represents the cutoff frequency and  $r$  represents a fractional order ranging from 0 to 2.

The PI controller  $G_f(s)$  is used to enlarge the slope of the amplitude curve in the low frequency range to be close to  $-40\text{dB/dec}$ . Similarly, the BICO filter is used to enlarge the slope of the amplitude curve in the high frequency range to be close to  $-40\text{dB/dec}$ .

Setting  $r = 1$ ,  $\omega_{cf} = 100\text{rad/s}$  as an example, the Bode plot of the BICO filter is compared with that of a normal first order low-pass filter in Fig. 3. According to Fig. 3, the magnitude roll-off of the BICO filter is much steeper. Meanwhile, the phase of the BICO filter is flat beyond the cut-off frequency.

Taking (6) as the open-loop transfer function of the control system, an improved BITF based controller is derived,

$$C(s) = G_f(s) \frac{b\omega_c^\xi}{K} \frac{1}{s^{\xi-\beta}} \left( 1 + \frac{c}{bs^\beta} + \frac{a}{b}s^{\alpha-\beta} \right) G_{\text{BICO}}(s). \quad (9)$$

Given the values of  $T_1$ ,  $\omega_{cf}$  and  $r$ , the PI controller  $G_f(s)$  and the BICO filter  $G_{\text{BICO}}(s)$  can be obtained. The phase of the open-loop control system at  $\omega_c$  is modified as

$$\text{Arg}[L(j\omega_c)] = \text{Arg}[G_f(j\omega_c)] + \pi \left( 1 - \frac{\xi}{2} \right) + \text{Arg}[G_{\text{BICO}}(j\omega_c)]. \quad (10)$$

Therefore, due to the introduction of  $G_f(s)$  and  $G_{\text{BICO}}(s)$ , the fractional order  $\xi$  is modified as

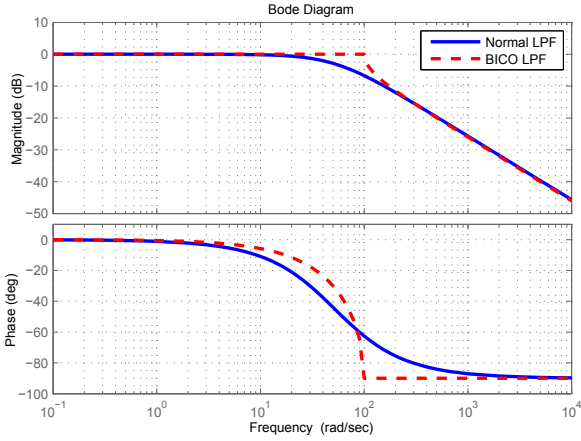


Fig. 3. The open Bode plot of the BICO low-pass filter and the normal low-pass filter

$$\xi = 2 \left( 1 - \frac{\varphi_m}{\pi} \right) + 2 \left( 1 + \frac{\text{Arg}[G_f(j\omega_c)] + \text{Arg}[G_{\text{BICO}}(j\omega_c)]}{\pi} \right). \quad (11)$$

Given the same design indices, an improved BITF based controller and an existing BITF based controller are designed for the lab-used PMSM speed servo system. The amplitude curves of the improved BITF based control system and the existing one are plotted in Fig. 4, respectively. It can be seen that, the amplitude curve of the system using the improved BITF based controller has larger declining slope than that using the existing BITF based controller in the low and high frequency ranges. Thus, applying the improved BITF based controller, the steady-state accuracy and disturbance rejection performance of the control system can be improved.

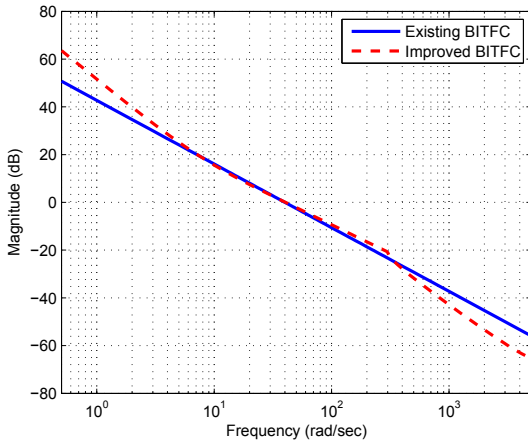


Fig. 4. The open-loop amplitude characteristics of the control systems using the existing and improved BITF based controllers

### 3. SIMULATION STUDY

The improved BITF based controller is applied to the lab-used PMSM speed servo system. Motor speed control simulation is performed to test the gain robustness, step response and anti-load disturbance performance of the improved BITF based control system. Besides, the response

of the improved BITF based control system is compared with those obtained using some existing methods.

The PMSM speed servo plant model can be represented as (3). Applying an output-error based modeling method (Zheng et al. (2016)), the transfer function of the lab-used PMSM plant model is obtained,

$$G(s) = \frac{4.74}{s(0.0127s + 1)}. \quad (12)$$

#### 3.1 Robustness study

Setting the integral time constant  $T_1$  as 0.2s, the PI controller is obtained,

$$G_f(s) = 1 + \frac{1}{0.2s}. \quad (13)$$

Setting the cutoff frequency  $\omega_{cf}$  as 300rad/s and order  $r$  as 0.757, the BICO filter is also obtained,

$$G_{\text{BICO}}(s) = \frac{1}{\left( \sqrt{1 + \left( \frac{s}{300} \right)^2} + \frac{s}{300} \right)^{0.757}}. \quad (14)$$

Given the design indices  $\omega_c = 35\text{rad/s}$ ,  $\varphi_m = 55^\circ$ , an improved BITF based controller is designed for the lab-used PMSM speed servo system,

$$C_1(s) = \frac{0.2s+1}{0.2s} \left[ \frac{17.528}{s^{0.242}} (1 + 0.0127s) \right] \frac{1}{\left[ \sqrt{1 + \left( \frac{s}{300} \right)^2} + \frac{s}{300} \right]^{0.757}}. \quad (15)$$

The open-loop Bode plot of the control system using the improved BITF controller is shown in Fig. 5. It can be seen that, the phase of the open-loop control system is close to a constant in the middle frequency range around  $\omega_c$ . In this way, when the gain of the control system has tiny variation, the change of the phase margin is small. Therefore, the overshoots of the step responses of the control systems with gain variation will be close to that of the system with the nominal gain.

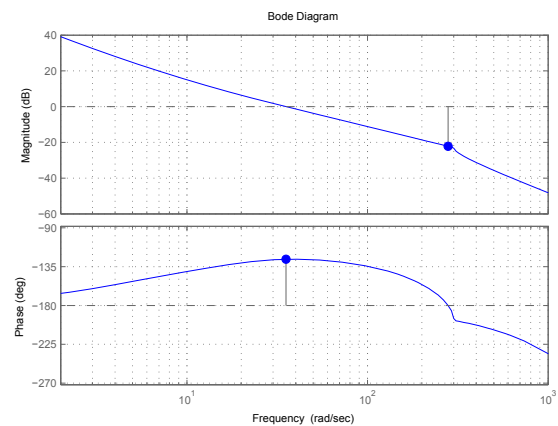


Fig. 5. The open-loop Bode plot of the control system using the improved BITF controller

Simulation is performed to verify the gain robustness of the improved BITF based control system. The plant model's gain is multiplied by 1.2 and 0.8 to simulate the

systems with gain variation. Step response simulation is performed on the motion control simulation platform. The step responses of the control systems with gain variation and the nominal system are plotted in Fig. 6.

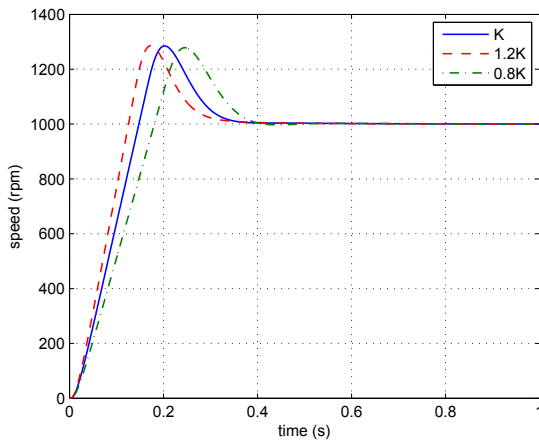


Fig. 6. The step responses of the improved BITF based control systems with gain variation

According to Fig. 6, the overshoots of the responses of the systems with gain variation are close to that of the nominal system. Therefore, the gain robustness of the control system is achieved.

### 3.2 Comparison with the existing BITF based controller

The dynamic performance of the improved BITF based control system is compared with that of the existing BITF based control system. According to the same design indices ( $\omega_c = 35\text{rad/s}$ ,  $\varphi_m = 55^\circ$ ), a BITF based controller is designed using the existing method,

$$C_2(s) = \frac{29.528}{s^{0.389}} (1 + 0.0127s). \quad (16)$$

Step response simulation is performed and the improved and existing BITF based controller are used to control the motor speed. The step responses of the improved BITF based control system and the existing BITF based control system are plotted in Fig. 7. Besides, load disturbance simulation is also performed to test the anti-load disturbance performance of the improved and existing BITF based control systems. The load disturbance responses of two systems are plotted in Fig. 8.

According to Fig. 7, the overshoots of the responses of the two control systems are close to each other, but it takes longer time for the speed of the existing BITF based control system to reach steady state. On the other hand, according to Fig. 8, under the sudden load increase, it also takes longer time for the speed of the existing BITF based control system to recover to its original value. Therefore, the improved BITF based control system shows better step response and anti-load disturbance performance than the existing one.

### 3.3 Comparison with the fractional order $PI^\lambda$ controller

Performance comparison is performed between the improved BITF based control system and the fractional order

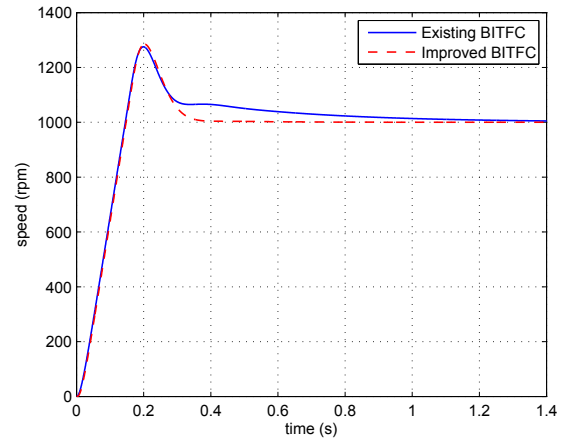


Fig. 7. The step responses of the existing BITF based control system (blue solid) and the improved BITF based control system (red dotted)

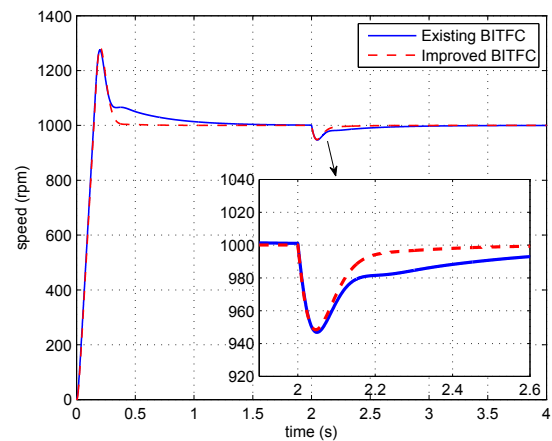


Fig. 8. The load disturbance responses of the existing BITF based control system (blue solid) and the improved BITF based control system (red dotted)

$PI^\lambda$  control system. To guarantee the fair comparison, the fractional order  $PI^\lambda$  controller is designed based on the same design indices as used by the improved BITF based controller, namely,  $\omega_c = 35\text{rad/s}$ ,  $\varphi_m = 55^\circ$ . Therefore, a fractional order  $PI^\lambda$  controller is designed using the commonly used “flat-phase” design method (Luo et al. (2010)),

$$C_3(s) = 9.955 \left( 1 + \frac{69.744}{s^{1.579}} \right). \quad (17)$$

Step response simulation is performed. The improved BITF based controller and the fractional order  $PI^\lambda$  controller are used to control the motor speed. The step responses of the improved BITF based control system and the fractional order  $PI^\lambda$  control system are plotted in Fig. 9. Besides, load disturbance simulation is also performed to test the anti-load disturbance performance of the improved BITF based control system and the fractional order  $PI^\lambda$  control system. The load disturbance responses of two systems are plotted in Fig. 10.

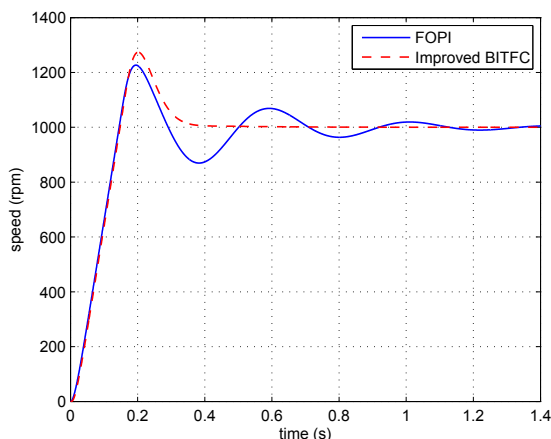


Fig. 9. The step responses of the fractional order  $PI^\lambda$  control system (blue solid) and the improved BITF based control system (red dotted)

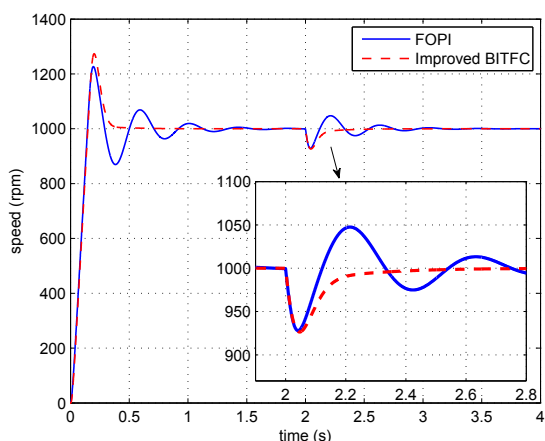


Fig. 10. The load disturbance responses of the fractional order  $PI^\lambda$  control system (blue solid) and the improved BITF based control system (red dotted)

According to Fig. 9, though the overshoot of the response of the improved BITF based control system is larger than that of the fractional order  $PI^\lambda$  control system, the oscillation is much smaller. Because of the large oscillation, the response of the fractional order  $PI^\lambda$  control system takes much longer time to reach the steady state. Beside, according to Fig. 10, under the sudden load increase, the speed of the fractional order  $PI^\lambda$  control system shows larger oscillation during the process where it recovers to its original value. As a result, the speed of the fractional order  $PI^\lambda$  control system recovers to its original value slower than that of the improved BITF based control system. Therefore, the improved BITF based control system shows better step response performance and anti-load disturbance performance than the fractional order  $PI^\lambda$  control system.

### 3.4 Comparison with a kind of IMC-PID controller

Performance comparison is performed between the improved BITF based control system and a kind of PID control system based on the internal mode control (IMC).

A common structure of the IMC-PID controller is composed of a PID controller and a filter. An IMC-PID controller is designed by setting the gain crossover frequency  $\omega_c = 35\text{rad/s}$ ,

$$C_4(s) = \frac{1}{0.0026s + 0.101} (1 + 0.0127s). \quad (18)$$

Step response simulation is performed. The improved BITF based controller and the IMC-PID controller are used to control the motor speed. The step responses of the improved BITF based control system and the IMC-PID control system are plotted in Fig. 11. Besides, load

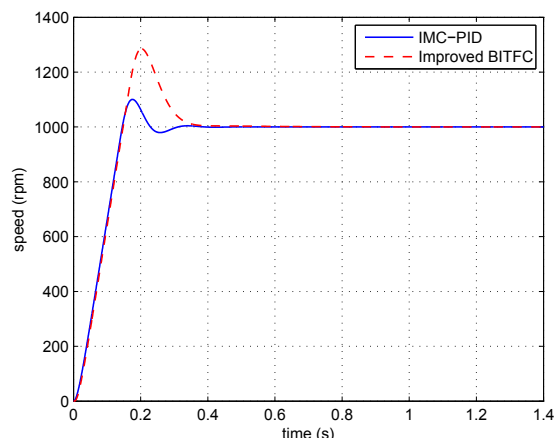


Fig. 11. The step responses of the IMC-PID control system (blue solid) and the improved BITF based control system (red dotted)

disturbance simulation is also performed to test the anti-load disturbance performance of the improved BITF based control system and the IMC-PID control system. The load disturbance responses of two systems are plotted in Fig. 12.

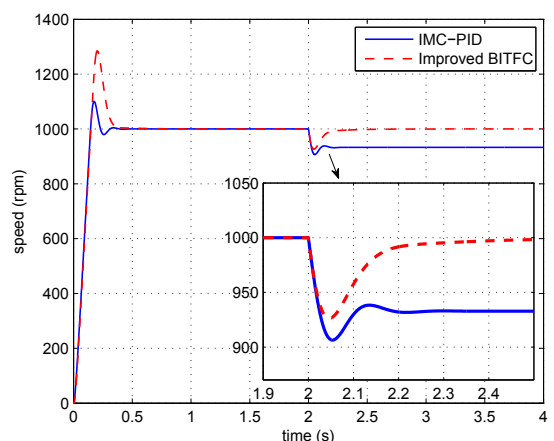


Fig. 12. The load disturbance responses of the IMC-PID control system (blue solid) and the improved BITF based control system (red dotted)

According to Fig. 11, the overshoot of response of the IMC-PID control system is smaller than that of the improved BITF based control system. On the other hand,

according to Fig. 12, the speed of the IMC-PID control system cannot recover to its original value after the load increase. On the contrary, the speed of the improved BITF based control system recovers to its original value in a short time. Therefore, though the IMC-PID control system achieves better step response performance, its anti-load disturbance performance is unacceptable. The improved BITF based control system shows better anti-load disturbance performance than the IMC-PID control system.

#### 4. CONCLUSION

An improved fractional order controller based on the Bode's ideal transfer function is proposed. Through the introduction of a PI controller and a BICO filter, the frequency characteristics of the control system in the low and high frequency ranges are improved, while the characteristic in the middle frequency range is reserved. Thus, applying the improved BITF based controller, the steady-state accuracy and anti-disturbance performance of a class of motion control systems can be improved. A tuning method for the improved BITF based controller is proposed. Thus, the controller parameters can be calculated analytically according to design indices. Motor speed control simulation is performed to test the dynamic performance of the improved BITF based control system. According to the simulation results, the improved BITF based control system shows better anti-load disturbance performance over those obtained using some existing methods.

#### ACKNOWLEDGEMENTS

This work is supported by the Natural Science Foundation of Guangdong, China (grant no. 2019A1515110180, 2017A030310580), the Foundation for Youth Innovation Talents in Higher Education of Guangdong, China (grant no. 2017KQNCX215), the National Natural Science Foundation of China (grant no. 61803086, 61803087, 61703104), the Science and Technology Planning Project of Guangdong, China (grant no. 2016B090911003) and Guangzhou Science and Technology Plan Project (grant no. 201902010066).

#### REFERENCES

Al-Saggaf, U.M., Mehedi, I.M., Mansouri, R., and Betayeb, M. (2016). State feedback with fractional integral control design based on the Bode's ideal transfer function. *Int J Syst Sci*, 47(1), 149–161.

Azarmi, R., Tavakoli-Kakhki, M., Sedigh, A.K., and Fatehi, A. (2016). Robust fractional order PI controller tuning based on Bode's ideal transfer function. In *IFAC Paperonline of the 6th IFAC Symposium on System Structure and Control (SSSC)*, volume 49, 158–164. IFAC, Istanbul, Turkey.

Bigdeli, N. (2015). The design of a non-minimal state space fractional-order predictive functional controller for fractional systems of arbitrary order. *J Process Contr*, 29, 45–56.

Bode, H.W. (1945). *Network Analysis and Feedback Amplifier Design*. Van Nostrand, New York.

Li, Z., Liu, L., Dehghan, S., and Chen, Y. (2017). A review and evaluation of numerical tools for fractional calculus

and fractional order controls. *Int J Control*, 90(6), 1165–1181.

Luo, Y., Chen, Y., Wang, C., and Pi, Y. (2010). Tuning fractional order proportional integral controllers for fractional order systems. *J Process Contr*, 20(7), 823–831.

Luo, Y., Zhang, T., and Lee, B. (2013). Disturbance observer design with Bode's ideal cut-off filter in hard-disc-drive servo system. *Mechatronics*, 23(7), 856–862.

Malek, H., Dadras, S., and Chen, Y. (2016). Fractional order equivalent series resistance modelling of electrolytic capacitor and fractional order failure prediction with application to predictive maintenance. *IET Power Electron*, 9(8), 1608–1613.

Monje, C., Vinagre, B., Feliu, V., and et al (2008). Tuning and auto-tuning of fractional order controllers for industry applications. *Control Eng Pract*, 16(7), 798–812.

Padula, F. and Visioli, A. (2011). Tuning rules for optimal PID and fractional-order PID controllers. *J Process Contr*, 21(1), 69–81.

Patil, D., Patil, M., and Vyawahare, V. (2015). Design of fractional-order controller for fractional-order systems using Bode's ideal loop transfer function method. In *Proc. of the International Conference on Industrial Instrumentation and Control (ICIC)*, 490–495. IEEE, Pune, India.

Podlubny, I. (1999). Fractional-order systems and  $PI^\lambda D^\mu$  controllers. *IEEE T on Automat Contr*, 44(1), 208–214.

Shah, P. and Agashe, S. (2016). Review of fractional PID controller. *Mechatronics*, 38, 29–41.

Tian, J., Xiong, R., and Yu, Q. (2019). Fractional-order model-based incremental capacity analysis for degradation state recognition of lithium-ion batteries. *IEEE T Ind Electron*, 66(2), 1576–1584.

Yumuk, E., Guzelkaya, M., and Eksin, I. (2019). Analytical fractional PID controller design based on Bode's ideal transfer transfer function plus time delay. *ISA T*, 91, 196–206.

Zheng, W., Luo, Y., Chen, Y., and Pi, Y. (2016). Fractional-order modeling of permanent magnet synchronous motor speed servo system. *J Vib Control*, 22(9), 2255–2280.